ISSN 2070-2051, Protection of Metals and Physical Chemistry of Surfaces, 2016, Vol. 52, No. 2, pp. 316–322. © Pleiades Publishing, Ltd., 2016.
Original Russian Text © M.V. Koteneva, S.A. Nikulin, A.B. Rozhnov, A.V. Kydryashova, 2016, published in Fizikokhimiya Poverkhnosti i Zashchita Materialov, 2016, Vol. 52, No. 2, pp. 223–230.

PHYSICOCHEMICAL PROBLEMS OF MATERIALS PROTECTION

The Influence of Oxidizing Medium on Structure, Mechanical Properties, and Breakage Pattern of Oxide Films of Zr–1% Nb Alloy under Conditions Simulating Oxidizing Media of WWER and PWR Reactors

M. V. Koteneva, S. A. Nikulin, A. B. Rozhnov, and A. V. Kydryashova

National University of Science and Technology (MISiS), Moscow, 119049 Russia

e-mail: mariakt@yandex.ru

Received February 1, 2015

Abstract—This article investigates into the structure, phase composition, mechanical properties, and breakage pattern of oxide films formed on the surface of Zr–1% Nb alloy after corrosion tests in autoclave in water, steam, and water with lithium. Oxidation in water with lithium promotes formation of oxide films with a thickness of more than 100 μm, and, after oxidation in water or steam, the thickness is 5–15 μm. Upon oxidation in water, oxide films are generated with laminar structure: in the substrate, the grains are extended with the thickness of ~80 nm, near film surface the grains are equiaxial with the diameter of ~30 nm. After holding of the specimens in steam the oxide films are comprised mainly extended grains with the thickness of ~95 nm with a minor amount of equiaxial grains, 10%, with a diameter of ~30 nm, after oxidation in water with lithium the mixture of equiaxial and weakly extended nanograins is observed in the film structure. Upon loading of specimens with the structure of equiaxial and weakly extended grains the oxide films are broken due to generation of transversal cracks propagating to basic metal. The oxide films with laminar structure oxidized in water are broken due to exfoliation along the interface between the layers of extended and equiaxial grains. Breakage of films with the structure of equiaxial and weakly extended grains starts at the stage of elastic deformation at a stress of 300 MPa. The highest breakage stresses of 1150 MPa are characteristic for alloy specimens oxidized in steam. Breakage of films with laminar structure after oxidation in water occurs at average stresses of 798 MPa. The cohesive/adhesive strengths of films oxidized in water and steam are nearly the same. In thick alloys, oxide films oxidized in water with lithium, substrate does not open even at loading of 100 N. According to data of Raman spectroscopy, oxide film is mainly comprised of monoclinic phase of zirconium oxide; however, after oxidation in steam at the metal–film interface, a barrier layer of tetragonal phase of zirconium dioxide has been detected that prevents accelerated oxidation.

DOI: 10.1134/S2070205116020155

INTRODUCTION

One of the main challenges of Russian and Western nuclear power engineering is the provision of high operational reliability of nuclear fuel elements and structures of nuclear fuel assemblies of high-duty reactors with increased fuel cycles and achievement of burn-up range of ⩾70 MW day/kg U. In this regard, alloys designed for the shells of nuclear fuel elements should provide high corrosion resistance and deformation resistance [1].

Zirconium alloys are widely applied as materials of structural elements of active areas of nuclear power reactors mainly for fabrication of the shells of nuclear fuel elements and other items of nuclear fuel assemblies. The main advantages of zirconium and its alloys are a low neutron capture cross section, high corrosion resistance, and rather high mechanical strength [2].

In the course of corrosion, depending on the chemical composition of an alloy, surface state, oxidation conditions, and type of oxidizing media, oxide films with various structures and surface imperfections are generated, which can significantly influence the protective properties and, finally, corrosion resistance of alloys.

The most conventional oxidizing media applied in various reactors are water, steam (in WWER) and water with lithium in PWR. The behavior of zirconium alloys under more severe operational conditions, related with increase in reactor power, burn-up range, including increase in LiOH content in water for PWR, is being investigated.

Lithium in PWR is used for maintaining of coolant pH in the range of 7.2 and 7.4. Corrosion resistance of zirconium alloys after oxidation in water and steam varies insignificantly. However, in the presence of lith-

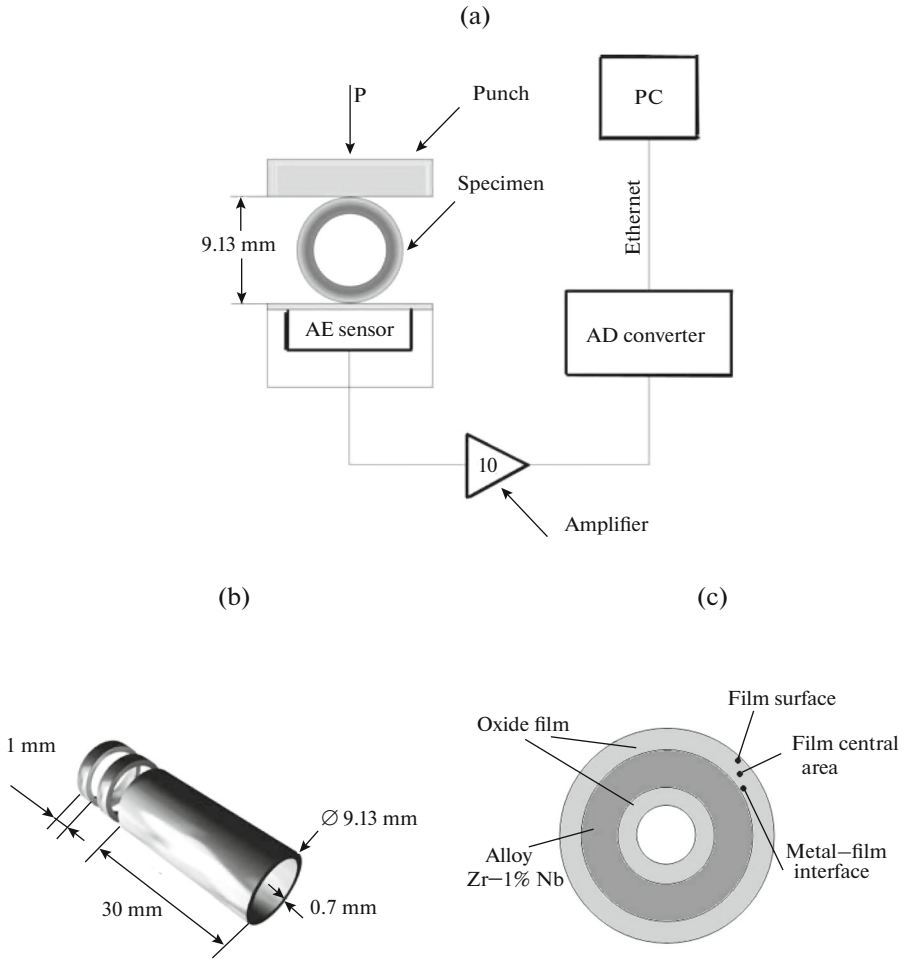

Fig. 1. Loading pattern and recording of acoustic emission signals (a) upon testing of annular specimens (b) with oxide films; (c) area of analysis of microstructure of oxide films by TEM and Raman spectroscopy.

ium in water, the oxidation rate within a certain time range sharply increases and nodular corrosion can occur [1].

Lithium content in an amount of several tens of ppm increases the oxidation rate after a preset operation lifetime. Zr–1% Nb, Zr–2.5% Nb alloys corrode intensively with sharp drop in corrosion kinetics. Sharp corrosion increase is observed in water containing 35 ppm of lithium at 360 after 90 days [3].

For Zircaloy 4, upon oxidation in medium with lithium content of 70 ppm at 633 K, a sharp increase in corrosion rate occurs in 100 days, and at lithium content of 700 ppm it does so after only a few days [4]. It is thought that, up to a sharp increase in the oxidation rate, tetragonal zirconium oxide is present on the internal film surface. Indeed, the corrosion rate increases, and when the oxidation rate is maximum, tetragonal phase in the film disappears.

The dense internal barrier layer of the film controls the corrosion rate and hinders lithium penetration. The structure of this layer is composed of extended grains with good cohesion. When the barrier layer degrades, lithium obtains access to metal; after some time, the internal layer disappears and, herewith, the corrosion rate increases. The structure of the new internal layer is composed of equiaxial grains, such structure provides access of lithium to metal [5].

Recently, in [6, 7], generation of oxide films in various conditions has been described in E110 and E635 zirconium alloys with various structure and resistance against breakage.

This work is aimed at an investigation of the influence of oxidation medium on the structure, phase composition, mechanical properties, and breakage pattern of oxide films of Zr–1% Nb alloy under con-

ditions simulating oxidizing media of WWER and PWR reactors.

EXPERIMENTAL

The investigations were performed with specimens of Zr–1% Nb alloy on an electrolytic base cut out of shell tubes with diameters of 9 and 13 mm and with a wall thickness of 0.7 mm (Fig. 1). Corrosion tests of all specimens were carried out in an autoclave in water, steam, and water with addition of lithium (Table 1). Upon testing in various media, oxide films with a thickness from 10 to 150 μm were generated on alloy specimens.

Microstructure of oxide films was studied on annular specimens by transmittance electron microscopy (TEM) and on polished cross sections by scanning electron microscopy (SEM). Preparation of specimens for TEM was carried out on field-ion microscope applying focused ion beam for etching of lamella (thin plate) from the specimen surface. Analysis of film structure by TEM was performed in two areas of oxide film: near the film surface and near the metal–film interface. Analysis of microstructure by SEM was performed on transversal polished cross sections.

Phase composition in two areas of oxide film, near film surface and near metal–film interface, was controlled by Raman probe spectroscopy using an AvaRaman-532 spectrometer equipped with an AvaRaman-PRB-FC-532 fiber optical probe with possibility of focusing of exciting radiation. Spectra were recorded at exciting wave length λ_{excit} = 532 nm and laser power of 50 mW in the range of 160–460 cm^{-1}. A specimen was placed onto the micrometric table with focusing possibility of a probing beam of exciting Raman scattering (RS) of laser radiation on external surface of oxide film, as well as in the surface area with locally removed oxide film. Film phase compositions of spectra were identified by comparison of the obtained RS spectra with known and reference RS spectra of certain oxides and RS spectra of Zr-oxide films [8].

In order to study accumulation of damages and breakages of oxide films upon deformation oxidized annular specimens with the height of 1 mm were compressed on universal testing apparatus with an INSTRON 5569 at loading rate of 0.1 mm/min with simultaneous measurement of acoustic emission (AE) (Fig. 1). AE signals were recorded by an R50I Physical Acoustics Corp. (PAC) sensor with a diameter of 29 mm and a height of 30 mm with an integral preamplifier.

Signals from the sensor were transferred to a PXI 1042 National Instruments (NI) analog-to-digital converter (ADC) via a Physical Acoustics Corp. (PAC) 2/4/6 amplifier with coefficient of amplification K_{amp} = 10. A receiver–amplifier of analog path processed input AE signals in the frequency range of 100–1200 kHz and a dynamic range of AE peak amplitudes up to 5 M. Digitized signals were transferred to a PC. The level of self-noise normalized to input in the working frequency range was U_{noise} ~ 30 mV, and the signal threshold was U_{TH} = 100 mV.

Table 1. Oxidation conditions of Zr–1% Nb alloy

Condition of specimens	Oxidation conditions	Thickness of oxide film, μm
1	Water T = 360°C, P = 18.6 MPa, t = 600 days	7 ± 1
2	Steam T = 400°C, P = 10.5 MPa, t = 300 days	14 ± 1
3	Water with addition of Li ~ 70 ppm T = 360°C, P = 18.6 MPa, t = 120 days	150 ± 5

Signal processing and analysis of AE diagrams were aided by the LabVIEW development environment of information and measuring system [9].

Deformation and AE diagrams, recorded during tests, were overlapped by time marks. The time of crack origination in oxide films was determined by AE pulses with amplitudes significantly higher than the noise level and by direct observation of crack origination on transversal polished cross sections of specimens using an optical microscope. Herewith, film breaking stresses σ_{br} and specimen deformations ε_{br} were measured at the time of crack origination in the film.

The adhesion/cohesion strength of oxide films was determined using a REVETEST scratch tester (CSM, Switzerland) by scratching an analyzed surface with a diamond cone indentor of Rockwell type upon continuously increasing loading.

RESULTS AND DISCUSSION

Surface analysis of considered tubular specimens of Zr–1% Nb alloy revealed that, after corrosion tests in water and steam, they were covered with smooth oxide films of black color, and after tests in the medium with lithium with loose films of white color. The thickens of oxide films after oxidation in water and steam equaled to 5–20 μm, and after oxidation in water with lithium to 150 μm.

The structure of oxide films varies depending on oxidizing medium. Detailed TEM analysis of microstructure of all specimens (Fig. 2) made it possible to highlight three main types of characteristic grain struc-

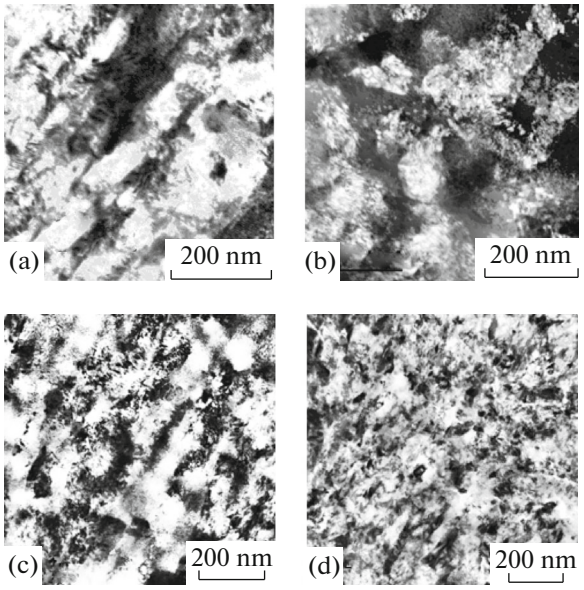

Fig. 2. TEM analysis of oxide films of Zr–1% Nb alloy oxidized in water (a) near substrate and (b) surface of films, oxidized in (c) steam and (d) in medium with lithium (across total film thickness.

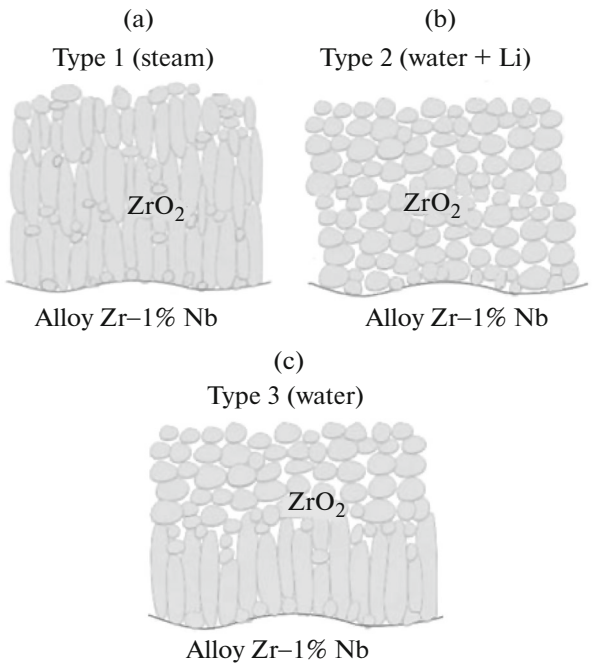

Fig. 3. Identified structure types of oxide films of zirconium alloys: (a) predominantly extended, (b) predominantly equiaxial, and (c) laminar.

tures of oxide films (Fig. 3): with predominantly extended grains (Type 1), with predominantly equiaxial grains (Type 2), and with laminar structure (Type 3).

After autoclave tests in water, oxide films with a laminar structure (Type 3) were generated (Fig. 3c): the substrate has extended grains with an average thickness of ~80 nm (Fig. 2a), while near the film surface the grains are equiaxial with an average diameter of ~30 nm (Fig. 2b).

After tests of specimens in steam, the oxide films are comprised mainly of extended films (Type 1) (Fig. 3a) with an average thickness of ~95 nm with a minor amount of equiaxial grains, 10%, with an average diameter of ~30 nm (Fig. 2c).

After oxidation in water with lithium, the alloy specimens were covered with films with a structure of Type 2 (Fig. 3b) comprised of a mixture of extended grains with an average thickness of ~47 nm and equiaxial grains with the average diameter of ~38 nm; herewith, the content of equiaxial grains increased toward the substrate (Fig. 2d).

SEM analysis of transversal polished cross sections with oxide films revealed existence of longitudinal cracks, parallel to the surface of oxide film (Fig. 4). The cracks of the minimum length of 1.4 ± 0.1 μm were detected in the films of alloy specimens (Table 2) oxidized in water, the cracks of the maximum length of 6.2 ± 0.8 μm were observed in films after oxidation in water with lithium. The crack length in films after oxidation in steam equaled to 3.1 ± 0.4 μm.

Investigation of the phase composition of oxide film using Raman scattering spectroscopy revealed correspondence of spectra shapes from both interfaces (from surface of oxide film and from surface layer at the metal–film interface for specimens of states 1 and 3 (Table 1) oxidized in aqueous media. According to the positions of spectral peaks, the oxide film was comprised mainly of a monoclinic phase of zirconium

Table 2. Quantitative properties of cracks in oxide films of Zr–1% Nb alloy

Properties	Conditions of specimens and oxidizing medium		
	1	2	3
	water	steam	water with lithium
Average film thickness, μm	7	14	150
Length of longitudinal cracks, μm	1.4 ± 0.1	3.1 ± 0.4	6.2
Density of cracks, 10^5 mm^{-2}	2 ± 0.1	5.3 ± 0.2	10.5 ± 0.5

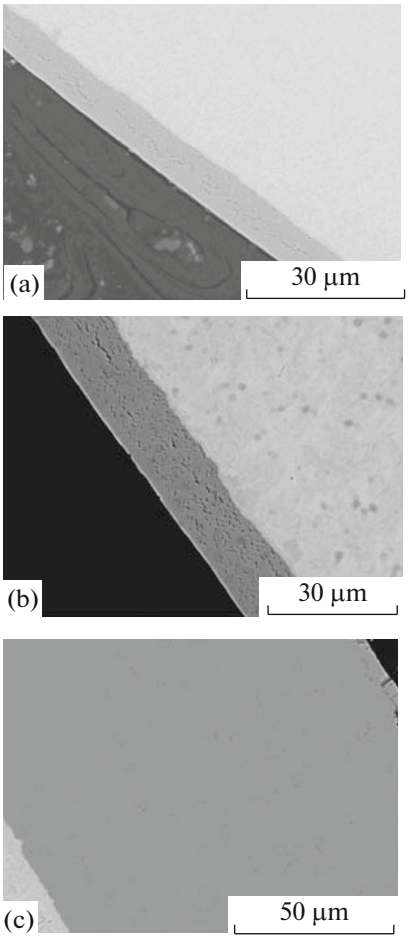

Fig. 4. Cracks in oxide films of Zr–1% Nb alloy oxidized in (a) water, (b) steam, and (c) medium with lithium.

oxide [8]. However, the alloy specimens after oxidation in steam showed significantly more pronounced peak 267.95 cm^{-1} from the metal–film interface in comparison with other specimens (Fig. 5a: band highlighted with an oval). Identification of this peak evidences existence of tetragonal phase near the metal–film interface [8]. The existence of tetragonal zirconium dioxide on internal interface makes it possible to assume that a barrier layer is present on a metal–film interface, which prevents accelerated oxidation (Fig. 5b). The nearly complete absence of tetragonal phase in specimens of other states evidences that allotropic transformation of tetragonal zirconium dioxide into a monoclinic one was completed.

Compression tests of annular oxidized specimens with recording of acoustic emission made enabled determination of breaking stress of oxide film σ_{br} and deformation of specimen ε_{br}, at which the film is broken.

The lower breaking stresses are characteristic for thick films with the structure of weakly extended and equiaxial grains in the alloy specimens oxidized in the medium with addition of lithium; herewith, the breakage occurs at the stress $\sigma_{br} = 300$ MPa and deformation of specimen $\varepsilon_{br} = 2\%$. Breakage of film starts at the stage of elastic deformation of specimen.

The highest breaking stress $\sigma_{br} = 1150$ MPa is characteristic for alloy specimens oxidized in steam, where film contains the structure comprised of extended grains. Generation of films with the structure comprised of long similarly oriented extended grains provides higher corrosion resistance in comparison with the structure with equiaxial or short extended grains [10, 11].

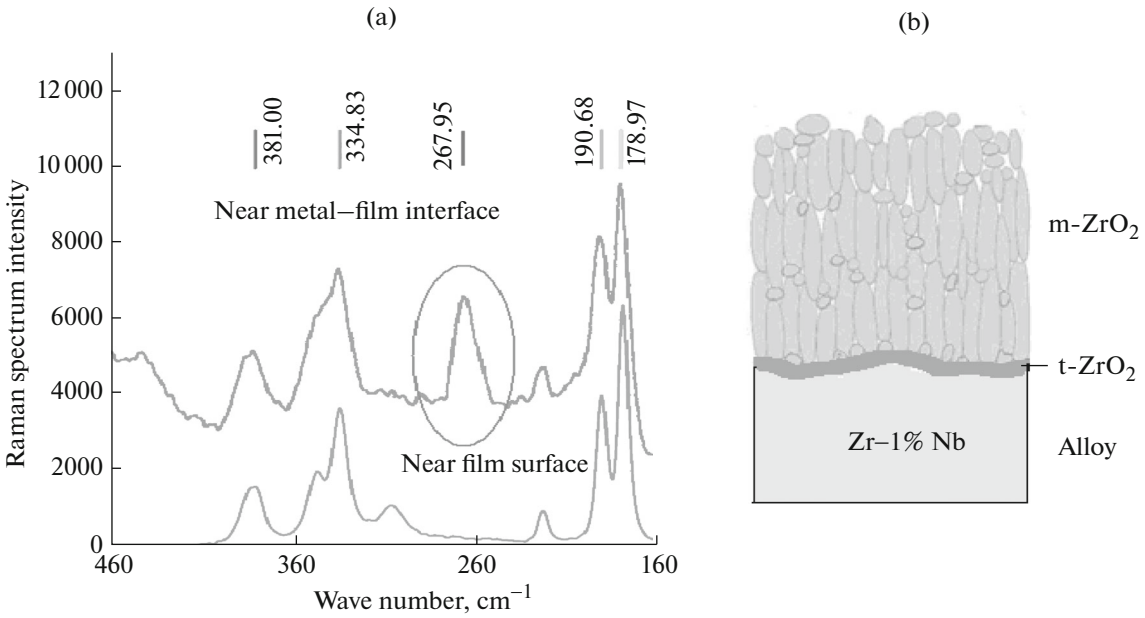

Fig. 5. (a) Raman spectrum and (b) structure of oxide film of Zr–1% Nb alloy oxidized in steam.

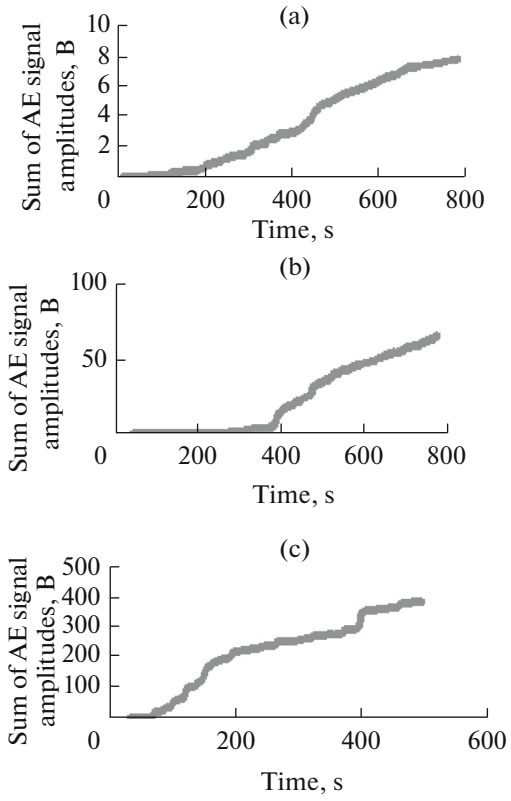

Fig. 6. Accumulation curves of AE signal amplitudes upon loading of Zr–1% Nb alloy oxidized in (a) water, (b) steam, and (c) medium with lithium.

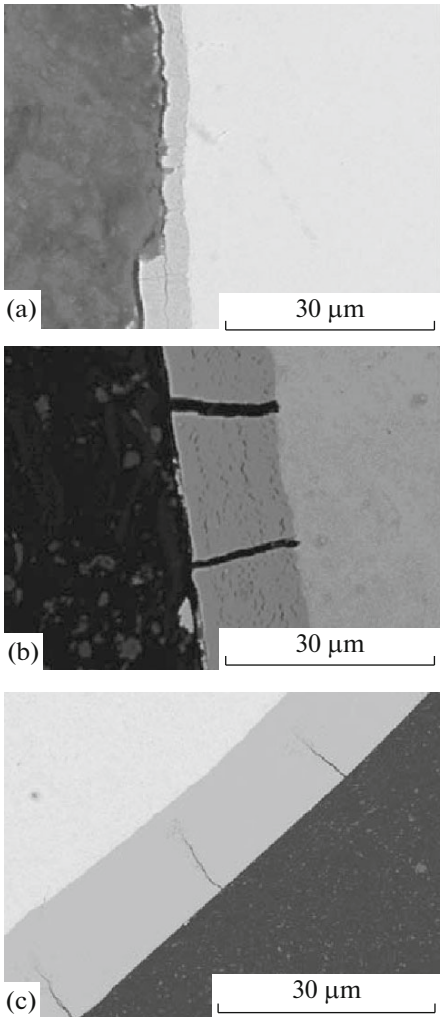

Fig. 7. Breakage of oxide films of Zr–1% Nb alloy upon loading by (a) exfoliation and (b, c) generation of transversal cracks.

Breakage of films with laminar structure after oxidation in water occurs at average stress $\sigma_{br} = 798$ MPa and deformation of specimen $\varepsilon_{br} = 4\%$.

Combined analysis of AE diagrams and deformation diagrams demonstrated that breakage of oxide films of specimens oxidized in water and steam occurs only upon plastic deformation of specimen. After oxidation in water with lithium breakage occurs already at earlier stages of elastic deformation of specimens.

It can be seen in cumulative curves of acoustic emission (Fig. 6) that accumulation of defects in films upon loading of specimens oxidized in water with lithium starts already in 80 s after loading (Fig. 6c), and in the films of specimens oxidized in water and steam only in 200–400 s (Figs. 6a, 6b). Herewith, an increase in the amount and size of defects occurs most markedly in the films of specimens oxidized in the medium with lithium, which is evidenced by more intense increase in the sum of AE signal amplitudes with loading time (Fig. 6c).

Analysis of the film breakage pattern demonstrated that oxide films of the specimens oxidized in water are broken by exfoliation along the interface between extended and equiaxial grains (Fig. 7a). After oxidation of specimens in steam and water with lithium, the films are broken by generation of transversal cracks propagating to the basic metal, and then there occurs longitudinal exfoliation of film from the basic metal substrate (Figs. 7b, 7c).

Cohesive/adhesive strength differs for films generated in water, steam, and water with lithium. Upon scratching of alloy specimens oxidized in water, film breakage occurs in two stages: origination of cracks along the scratch edges and complete opening of substrate, which occurs at loadings of 3.8 and 15 N.

For alloy specimens oxidized in steam the origination of cracks along the scratch edges, local fracturing along the scratch edges takes place at 3.5 N, while opening of the basic metal substrate takes place at 17.8 N.

Therefore, the cohesive/adhesive film strength of specimens oxidized in water and steam varies insignificantly.

In thick oxide films of alloy specimens oxidized in water with lithium, a fracture near a scratch occurs at

3 N, and opening of substrate does not occur even at the loading of 100 N.

CONCLUSIONS

Upon oxidation in water with the addition of lithium, after only 120 days, oxide films of white color are generated with a thickness of 100–150 μm. After oxidation of a specimen of the same Zr–1% Nb alloy in water or steam, films of black color are generated with a thickness of 5–20 μm.

Oxidation in water with addition of lithium promotes generation of oxide film with the structure comprised of equiaxial and weakly extended grains. After oxidation in water the films with laminar structure are generated, and after oxidation in steam the structure is composed of extended grains.

Breakage of the oxide films upon loading of specimens, generated after oxidation in the medium with lithium, occurs under stresses of 300 MPa due to generation of transversal cracks perpendicular to film surface at the stage of elastic deformation of specimen. Breakage of films generated after oxidation in water or steam occurs at stresses that are two to five times higher upon plastic deformation of specimen.

ACKNOWLEDGMENTS

The work was supported by project no. 14.A12.31.0001 dated June 24, 2013.

We are grateful to OAO VNIINM for assistance in experiments, as well as to the Frumkin Institute of Physical Chemistry and Electrochemistry, Russian Academy of Sciences, for assistance in spectral measurements.

REFERENCES

1. Nikulina, A.V., Peregud, M.M., Kon'kov, V.F., Khokhunova, T.N., Sablin, M.N., and Mileshkina, O.Yu., *Tsirkonievye splavy, soderzhashchie niobii dlya TBS reaktorov VVER i PWR povyshennoi moshchnosti s dostizheniem vygoraniya topliva ⩾70 MVt·sutki/kgU* (Zirconium Alloys with Niobium for VVER Fuel Assemblies Reactor and PWR with the Higher Power Fuel Combustion ⩾70 MVt day/kgU), Moscow: Vseross. Nauchno-Issled. Inst. Neorg. Mater. im. A.A. Bochava, 2014, no. 1.
2. Zaimovskii, A.S., Nikulina, A.V., and Reshetnikov, N.G., *Tsirkonievye splavy v atomnoi energetike* (Implementation of Zirconium Alloys in Atomic Energetics), Moscow: Energoatomizdat, 1981.
3. Sabol, G.P., et al., Development of a cladding alloy for high burnup, in *Eight Int. Symp. Zirconium in the Nuclear Industry, ASTM STP 1354,* West Conshohocken, PA: Am. Soc. Test. Mater.,1989, vol. 1023, pp. 227–244.
4. Pecheur, D., et al., Contribution to the understanding of the effect of the water chemistry on the oxidation kinetics of Zircaloy-4 cladding, in *Twelfth Int. Symp. "Zirconium in the Nuclear Industry," ASTM STP 1354,* West Conshohocken, PA: Am. Soc. Test. Mater., 2000, no. 1354, pp. 793–811.
5. Pecheur, D., et al., Microstructure of oxide films formed during the waterside corrosion of the Zircaloy-4 cladding in litigated environment, in *Eleventh Int. Symp. "Zirconium in the Nuclear Industry,"* West Conshohocken, PA: Am. Soc. Test. Mater., 1996, no. 1295, pp. 94–112.
6. Koteneva, M.V., Nikulin, S.A., Rozhnov, A.B., and Kudryashova, A.V., Structure and kinetics of the destruction of oxide films formed on the samples of E110 alloy after different surface treatment, *Deform. Razrushenie Mater.,* 2015, no. 2, pp. 31–34.
7. Koteneva, M.V., Nikulin, S.A., Rozhnov, A.B., and Rogachev, S.O., Structure and mechanical properties of oxide films on zirconium alloys upon oxidation under different conditions, *Prot. Met. Phys. Chem. Surf.,* 2014, vol. 50, no. 1, pp. 64–68.
8. Maslar, J.E., Hurst, W.S., Bowers, W.J. Jr., and Hendrics, J.H., *J. Nucl. Mater.,* 2001, vol. 298, p. 239.
9. Nikulin, S.A. and Khanzhin, V.G., Monitoring of materials, processes, and technologies by measuring acoustic emission, *Met. Sci. Heat Treat.,* 1999, vol. 41, no. 4, pp. 174–181.
10. Garzarolli, F., Seidel, H., Tricot, R., et al., Oxide growth mechanism on zirconium alloys, in *IX Int. Symp. "Zirconium in the Nuclear Industry,"* 1991, vol. 1132, pp. 395–415.
11. Yilmazbayhan, A., et al., Transmission electron microscopy examination of oxide layers formed on Zr alloys, *J. Nucl. Mater.,* 2006, vol. 349, no. 3, pp. 265–281.

Translated by I. Moshkin